AGU PUBLICATIONS

Geophysical Research Letters

RESEARCH LETTER

10.1002/2015GL063726

Special Section:
Effects of the Comet C/2013 A1 (Siding Spring) meteor shower in 2014 on Mars atmosphere and ionosphere: Observations from MAVEN, Mars Express, and Mars Reconnaissance Orbiter

Key Points:
- Dust from comet Siding Spring causes dense ionization in the atmosphere of Mars
- The ionization was detected by the MEX radar ~7 h after closest approach
- The peak ionization density was ~2.5×10^5 cm^{-3} at an altitude of 80 to 100 km

Supporting Information:
- Texts S1–S3, Figures S1–S6, and Table S1

Correspondence to:
D. A. Gurnett,
donald-gurnett@uiowa.edu

Citation:
Gurnett, D. A., D. D. Morgan, A. M. Persoon, L. J. Granroth, A. J. Kopf, J. J. Plaut, and J. L. Green (2015), An ionized layer in the upper atmosphere of Mars caused by dust impacts from comet Siding Spring, *Geophys. Res. Lett.*, *42*, 4745–4751, doi:10.1002/2015GL063726.

Received 3 MAR 2015
Accepted 2 APR 2015
Published online 16 JUN 2015

An ionized layer in the upper atmosphere of Mars caused by dust impacts from comet Siding Spring

D. A. Gurnett[1], D. D. Morgan[1], A. M. Persoon[1], L. J. Granroth[1], A. J. Kopf[1], J. J. Plaut[2], and J. L. Green[3]

[1]Department of Physics and Astronomy, University of Iowa, Iowa City, Iowa, USA, [2]Jet Propulsion Laboratory, Pasadena, California, USA, [3]NASA Headquarters, Washington, District of Columbia, USA

Abstract We report the detection of a dense ionized layer in the upper atmosphere of Mars caused by the impact of dust from comet Siding Spring. The observations were made by the ionospheric radar sounder on the Mars Express spacecraft during two low-altitude passes approximately 7 h and 14 h after closest approach of the comet to Mars. During these passes an unusual transient layer of ionization was detected at altitudes of about 80 to 100 km with peak electron densities of (1.5 to 2.5) $\times 10^5$ cm^{-3}, much higher than normally observed in the Martian ionosphere. From comparisons to previously observed ionization produced by meteors at Earth and Mars, we conclude that the layer was produced by dust from the comet impacting and ionizing the upper atmosphere of Mars.

1. Introduction

Comet Siding Spring, officially designated C/2013 A1 by the International Astronomical Union, was discovered by *McNaught et al.* [2013] on 3 January 2013, at the Siding Spring Observatory in Coonabarabran, Australia. The initial observation was at a heliocentric radial distance of 7.2 AU (astronomical units). Subsequent analyses showed that the comet originated from the Oort cloud on a highly inclined, nearly parabolic, retrograde orbit that would pass very close to Mars at about 18:30 UT (universal time) on 19 October 2014. The closest approach distance was estimated to be about 135,000 km, at an approach velocity of 56 km s^{-1} [*Tricarico et al.*, 2014; *Farnocchia et al.*, 2014; *Kelley et al.*, 2014]. Because of the very high approach velocity, impacts of dust from the comet had the potential of causing major ionization in the upper atmosphere of Mars [*Withers*, 2014]. The arrival time of the cometary dust was estimated to occur about 90 to 100 min after closest approach [*Moorhead et al.*, 2014]. If solar heating caused the production rate of gas from the nucleus to exceed about 10^{28} to 10^{29} molecules/s, the coma gases also had the potential of causing significant heating and ionization effects, possibly lasting several hours or more [*Yelle et al.*, 2014; *Kelley et al.*, 2014].

2. The Mars Express Radar Sounder

Very early in the planning for the encounter, it was realized that the remote sensing capability of the Mars Advanced Radar for Subsurface and Ionospheric Sounding (MARSIS) instrument on the Mars Express spacecraft could provide crucial observations. Mars Express is in an eccentric near-polar orbit around Mars with a periapsis altitude of ~375 km, an apoapsis altitude of ~10,000 km, an inclination of ~86°, and an orbital period of ~7 h. MARSIS has two modes of operation, one for subsurface sounding and the other for ionospheric sounding [*Picardi et al.*, 2004]. Since significant ionization effects were expected, the ionospheric sounding mode was selected as the primary operating mode. In this mode the radar transmits a short pulse at a fixed frequency and then measures the time delay for the pulse to reflect from the ionosphere and return to the spacecraft. As shown in Figure 1, for vertical incidence the ionospheric reflections occur at the point in the ionosphere where the wave frequency is equal to the electron plasma frequency, $f_p = 8980\sqrt{n_e}$ Hz, where n_e is the electron density in cm^{-3}. By sequentially stepping the transmitter frequency through a range of frequencies, a vertical profile of the electron density in the ionosphere can be obtained. In the ionospheric mode the radar transmitter steps through 160 quasi-logarithmically spaced frequencies from 0.1 to 5.5 MHz in 1.26 s, and repeats this cycle once every 7.54 s [*Gurnett et al.*, 2005]. As a first-order approximation, the location of the reflection point can be calculated assuming that the radar pulse travels at the speed of light, in which case the altitude of reflection is called the apparent altitude. However, for precise measurements the effect of the plasma on the speed of

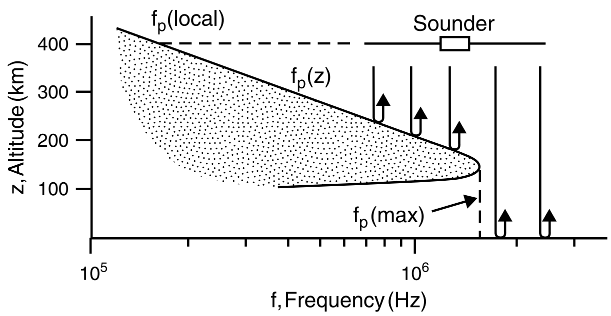

Figure 1. A representative profile of the electron plasma frequency, f_p, as a function of altitude, *z*, in the Martian ionosphere. Since radio waves cannot propagate at frequencies below the electron plasma frequency, radar pulses transmitted at a frequency, *f*, from the sounder are reflected at the altitude where $f = f_p$.

propagation must be taken into account. This effect is called dispersion. For a more detailed discussion of the sounder operation and the methods used to correct for dispersion, see Text S1 in the supporting information and also *Morgan et al*. [2013]. During the period around closest approach of the comet to Mars, the ionospheric radar soundings started at an altitude of about 1200 km over the nightside northern polar region, then proceeded almost directly southward across the nightside/dayside terminator, through periapsis at about 375 km, and ended at midlatitudes in the southern hemisphere at about 1200 km. The spacecraft trajectory in latitude/local time coordinates is shown in Figure 2.

3. Observations

Ionospheric sounder data are usually displayed in the form of an ionogram, which is a color-coded plot of the echo intensity as a function of frequency and time delay, see Text S2. To illustrate the radar observations obtained around the time of closest approach, the ionograms from five successive periapsis passes (orbits 13708 through 13712) are shown in Figure 3. In these ionograms the time delay has been converted to apparent altitude. The ionograms in the first column (Figure 3a) are from near point P1 over the nightside polar region of Mars (see Figure 2), and the ionograms in the second column (Figure 3b) are from near point P2 about 10 min later at midlatitudes on the dayside of Mars. Of these, the first evidence of anything unusual was on orbit 13,710, 7 h after closest approach. On this pass, strong radar echoes were observed at an apparent altitude of about 100 km over the nightside polar region at frequencies extending as high as 4.6 MHz (see Figure 3a, third row). The plasma frequency, f_p, at the highest reflection frequency corresponds to an electron density of $2.6 \times 10^5\,\mathrm{cm}^{-3}$. Such high densities have never previously been observed on the nightside of Mars. A few minutes later on this same orbit, similar radar echoes were detected on the dayside of Mars at frequencies extending well above the normal dayside ionosphere echoes (see

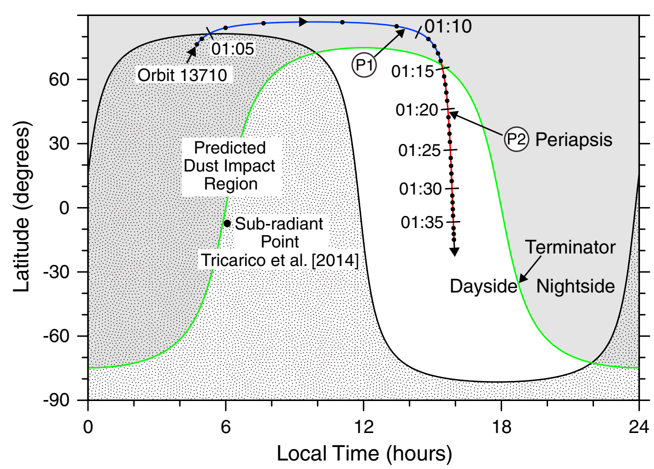

Figure 2. Mars Express trajectory during the Siding Spring encounter with Mars. The times shown on the subspacecraft track (dark line with arrows) are for orbit 13,710 where the main results were obtained. Other orbits around this time have almost the same track. The dotted region is where dust impacts from the comet were predicted to occur within 1–2 h after closest approach, and the shaded region is the nightside of the planet.

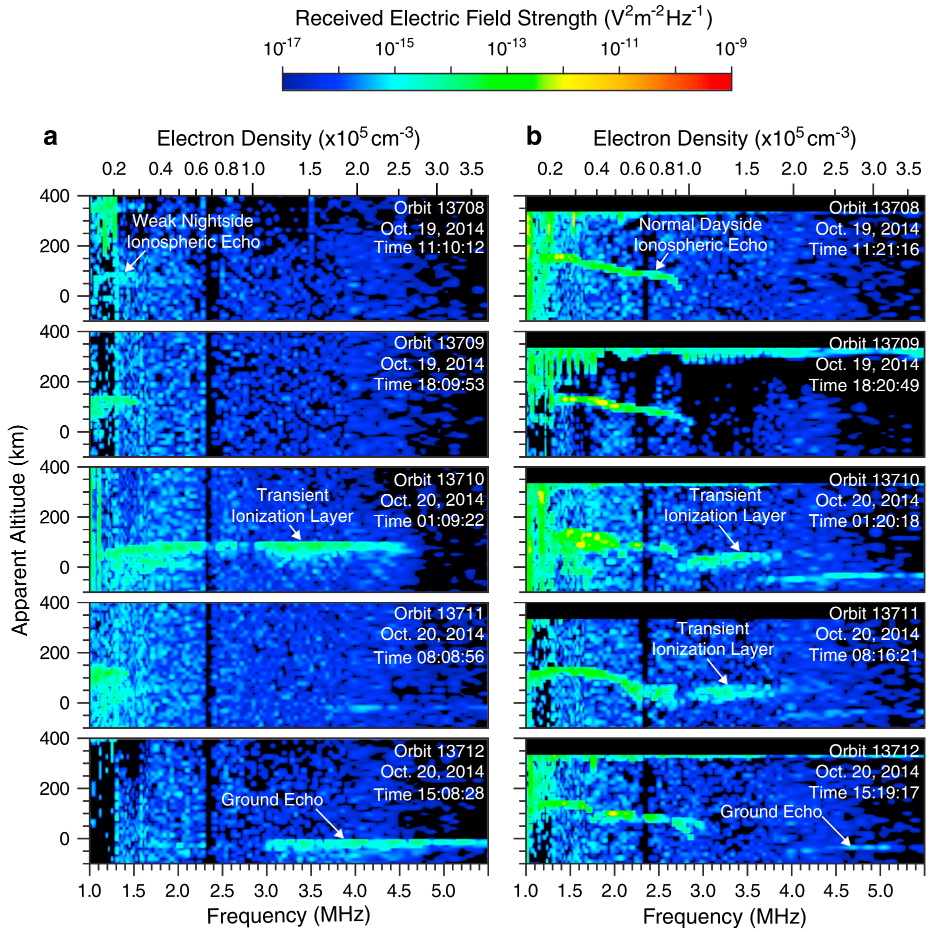

Figure 3. Representative ionograms for five Mars Express passes around the time of closest approach of the comet to Mars. (a) Ionograms over the northern nightside polar region (point P1 in Figure 2) showing the color-coded intensities of the received radar echoes. The frequency of the transmitted radar pulse is on the horizontal axis of each ionogram, and the apparent altitude of the resulting echoes is on the vertical axis. The apparent altitude assumes that the radar pulse propagates vertically at the speed of light, with no correction for plasma dispersion (see Text S1). Note the strong radar echoes from an ionized layer at an altitude of about 100 km extending up to about 4.6 MHz in the third row (orbit 13710). (b) Ionograms from the same series of passes (point P2 in Figure 2) near periapsis about 10 min after those in Figure 3a. Again strong radar echoes can be seen in the third row (orbit 13,710) and also on the fourth row (orbit 13,711). In both cases the echoes extend to frequencies well above the normal ionospheric echoes.

Figure 3b, third row). The highest reflection frequency in this case was about 3.8 MHz, corresponding to an electron density of about 1.79×10^5 cm^{-3}. On the next pass, orbit 13,711, approximately 14 h after closest approach, the enhanced ionization over the nightside polar region had completely disappeared, but there was still evidence of an enhanced ionization layer on the dayside of Mars (see Figure 3b, fourth row). On the final pass in the sequence, orbit 13,712, there was no evidence of the enhanced ionization layer. The highly unusual layer of enhanced ionization observed on orbits 13,710 and 13,711, with densities higher than ever previously observed over the nightside, and among the highest ever observed over the dayside, provides compelling evidence that the transient layer was caused by the comet.

The latitudinal sequence of ionograms in Figure 4 shows that on orbit 13,710 the transient ionization layer extended nearly continuously from the nightside polar region well into the dayside midlatitude region. The variations in the peak electron density of the transient layer and the normal ionosphere are shown in Figure 5a. The electron density of the transient layer was highly variable, ranging from about (1.5 to 2.5) $\times 10^5$ cm^{-3}, with two well-defined peaks, and two brief periods where no echoes were detected. In all cases the peak densities of the transient layer (blue dots) were well above the peak density of the Martian ionosphere (red dots). Measurements of the reflection altitude for the transient layer are shown in Figure 5b. These measurements are

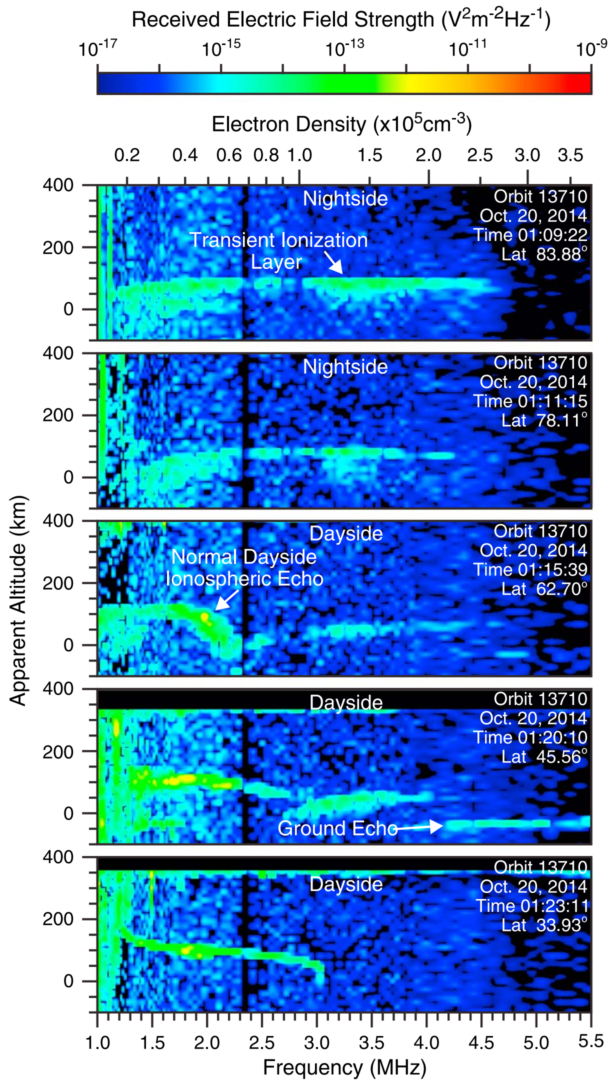

Figure 4. The latitudinal variation of the transient ionized layer. Five ionograms from orbit 13,710 showing the latitudinal variation of radar echoes from the transient ionized layer. In the first two ionograms, which are on the nightside, the apparent altitude of the reflecting layer is nearly independent of frequency, indicating a very sharply defined upper edge. A slight downward curvature due to plasma dispersion can be seen at frequencies below about 1.5 to 2 MHz. This dispersion is due to ionospheric plasma of very low densities between the spacecraft and the reflecting layer. In the third and fourth ionograms the dispersion effect becomes more apparent as the spacecraft moves into the dayside where the ionospheric plasma density starts to increase, as indicated by the onset of strong ionosphere echoes. In the fourth ionogram the dispersion due to the transient layer becomes even more pronounced. In the fifth (bottom) ionogram the transient ionized layer can no longer be detected.

somewhat complicated by plasma dispersion effects. On the nightside, before about 01:11 UT, where the ionospheric plasma density is so low that the propagation speed is essentially the speed of light, the reflection altitude was consistently around 100 ± 7 km, with a slight downward trend with increasing time. After about 01:11 UT, as the spacecraft moves into the dayside where the ionospheric density is rapidly increasing due to solar illumination, the uncorrected altitudes (black dots) start to decrease rapidly due to the increasing plasma dispersion. Attempts to correct for the dispersion in this region were of limited success due in part to the diffuse and highly disturbed ionospheric echoes present during this part of the pass. The relatively few dispersion-corrected altitudes that we did obtain (red dots) have considerable scatter but follow the same slightly downward trend as in the region where no corrections were necessary. The arrows at the bottom of Figure 5 show the location of ionograms in which ground echoes were observed. Note that there are very few

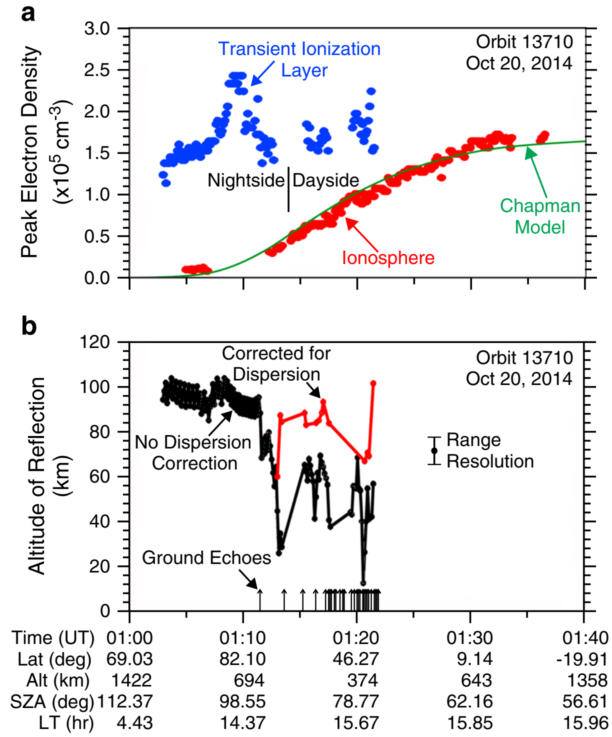

Figure 5. The electron density and reflection altitude of the transient ionized layer for orbit 13710. (a) The peak density of the transient ionization layer (blue), the peak density of the Martian ionosphere (red), and the best fit to the Chapman model (green) for planetary ionospheres [*Chapman*, 1931]. (b) The reflection altitudes of echoes from the transient ionization layer uncorrected for plasma dispersion (black), and corrected for plasma dispersion (red), both assuming vertical incidence. Before about 01:11 UT, no dispersion correction is necessary because ionospheric plasma density is so low in this region. The arrows at the bottom show that very few ground echoes were observed.

ground echoes over the nightside polar region, which was also the case for orbits 13,708 and 13,709, even before the arrival of the comet. However, note from the bottom ionogram of Figure 3a that very strong ground echoes have returned over the polar region on orbit 13,712. The absence of strong ground echoes even before the arrival of the comet, and the sudden return of strong ground echoes on orbit 13,712, 21 h after closest approach, indicates some type of radio wave absorption effect is occurring that is not related to the comet. The most likely origin of this variability is solar energetic particles that can produce ionization deep in the atmosphere where collisions cause strong absorption.

Inspection of ionograms obtained from orbit 13,711, 14 h after closest approach, revealed that the transient ionization layer was also detected over a very limited region, from 08:15:57 to 08:16:50 UT, on this pass. The ionogram in the fourth row of Figure 3b shows one of the few (eight) transient echoes observed in this region. Figure 6 shows the peak electron densities and reflection altitudes of the transient layer for orbit 13,711, in the same format as Figure 5. The electron densities and reflection altitudes are very similar to those observed on orbit 13,710. Note the distinct absence of ground echoes in the brief region where the transient ionization layer occurs. This anticorrelation suggests that the radar signal is being absorbed by collisional damping in the region of enhanced ionization, as has been predicted for meteor impacts in the Martian ionosphere by *Witasse et al*. [2001].

In addition to the altitude, the thickness of the ionized layer is also of considerable interest. Since radar echoes from the topside of the ionized layer do not pass through the layer, no measurements of the thickness can be obtained from the topside echoes. However, information on the thickness can be obtained from the ground echoes, since these signals pass through the layer twice (first downward and then upward). It can be shown (see Text S3) that the dispersion of the ground echoes gives a direct measurement of the column integral of the electron density from the ground to the spacecraft, called the total electron content, $TEC = \int n_e dz$. By subtracting the TEC of the ionosphere from the TEC of the ground echoes, the TEC of the transient layer can

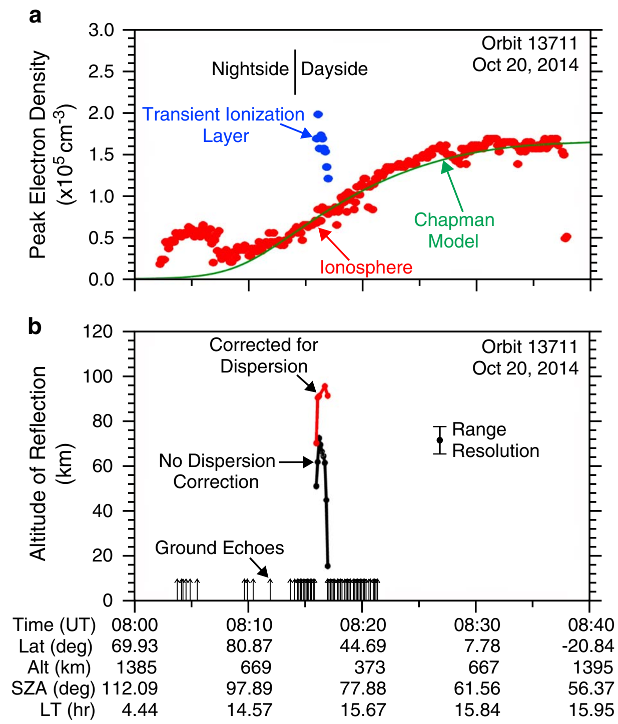

Figure 6. The electron density and reflection altitude of the transient ionized layer for orbit 13,711. (a) The peak density of the transient ionized layer (blue), the peak density of the Martian ionosphere (red), and the best fit to the Chapman model (green), in the same format as Figure 5. On this orbit, the transient ionization layer was observed only for a very brief interval (about 1 min) shortly before periapsis, see the fourth ionogram from the top in Figure 3b. (b) The reflection altitudes of echoes from the transient ionization layer uncorrected for plasma dispersion (black) and corrected for plasma dispersion (red). The arrows at the bottom show where ground echoes were observed.

be determined. The effective slab thickness of the layer can then be computed by dividing by the peak density of the transient layer. Unfortunately, of the available data, only three ionograms were found that have ground and ionospheric echoes sufficiently strong to provide reliable measurements of the thickness. The computed thicknesses ranged from 13.7 to 42.3 km (see Text S3). The larger of these thicknesses may be inconsistent with the observations of ground reflections due to the strong collisional absorption expected in the lower levels of the atmosphere. This inconsistency needs to be studied further, but a possible explanation might be that the ionization is patchy, which would allow some of the ground-reflected radar signals to be detected.

4. Conclusions

Of the two components, gas and dust, released from the comet, we have concluded that only dust can cause the transient layer of ionization reported here. The altitude of this layer, which has an upper limit of about 100 ± 7 km and extends downward by possibly as much as 40 km, is far below the altitudes where the primary interaction with cometary gas was expected, i.e., ~150 km, see *Yelle et al*. [2014]. On the other hand, the altitudes are in good agreement with the altitudes of the transient M3 layer in the Martian ionosphere, ~65 to 110 km, as reported by *Pätzold et al*. [2005]. The M3 layer is believed to be caused by the impact of meteors. Our conclusion is also supported by the observations from the MAVEN spacecraft of ionized magnesium, iron, and other meteoritic ablation products during this same time [*Benna et al*., 2015; *Schneider et al*., 2015].

It is interesting to note that the observations obtained here were taken over a local time region that was not exposed to direct impacts of dust from the comet (Figure 2). The main flux of meteoritic particles probably occurred 5 to 6 h before our earliest observations [*Tricarico et al*., 2014]. Evidence of the early arrival of the particles is given by the SHARAD radar on the Mars Reconnaissance Orbiter spacecraft, which detected greatly enhanced TECs as early as 3 h after closest approach [*Restano et al*., 2015]. The enhanced TECs lasted almost 10 h. This means that the ionization reported here had to be transported by the rotation of the Martian atmosphere from the main impact region over a period of 10 h, or more, and also in local time. That the ionization could have such long lifetimes is supported by both long-term radio occultation observations of the transient M3 layer [*Pätzold et al.*, 2005] and theoretical calculations showing that the photochemical lifetime of metallic ions produced by meteor impacts can be as long as 10 days or more [*Withers et al*., 2008].

Acknowledgments

All the data used in this study are available at http://www-pw.physics.uiowa.edu/marsx/Gurnett_etal_GRL_2015. The research at the University of Iowa was supported by NASA through contract 1224107 with the Jet Propulsion Laboratory. We thank the many members of the scientific, technical, and management teams at NASA Headquarters, the Jet Propulsion Laboratory, the European Space Agency, and the Italian Space Agency for their effort in planning the spacecraft operations required to successfully obtain these data.

The Editor thanks Zoltan Sternovsky and an anonymous reviewer for their assistance in evaluating this paper.

References

Benna, M., P. Mahaffy, J. Grebowsky, J. Plane, R. Yelle, and B. Jakosky (2015), Metallic ions in the upper atmosphere of Mars from the passage of comet Siding Spring, *Geophys. Res. Lett.*, doi:10.1029/2015GL064159.

Chapman, S. (1931), The absorption and dissociative or ionizing effect of monochromatic radiation in an atmosphere on a rotating Earth: Part II. Grazing incidence, *Proc. R. Soc. London*, *43*(26), 483–501, doi:10.1088/0959-5309/43/5/302.

Farnocchia, D., S. R. Chesley, P. W. Chodas, P. Tricarico, M. S. P. Kelley, and T. L. Farnham (2014), Trajectory analysis for the nucleus and dust of comet C/2013 A1 (Siding Spring), *Astrophys. J.*, *790*, 114–120, doi:10.1088/0004-637X/790/2/114.

Gurnett, D. A., et al. (2005), Radar sounding of the ionosphere of Mars, *Science*, *310*, 1929–1933, doi:10.1126/science.1121868.

Kelley, M. S. P., T. L. Farnham, D. Bodewits, P. Tricarico, and D. Farnocchia (2014), A study of dust and gas at Mars from comet C/2013 A1 (Siding Spring), *Astrophys. J. Lett.*, *792*, L16, doi:10.1088/2041-8205/792/1/L16.

McNaught, R. H., H. Sato, and G. V. Williams (2013), Comet C/2013 A1 (Siding Spring), in *Central Bureau Electronic Telegrams*, edited by D. W. E. Green, 3368, p. 1, Commission 6, International Astronomical Union, Cambridge, Mass.

Moorhead, A. V., P. A. Wiegert, and W. J. Cooke (2014), The meteoroid fluence at Mars due to Comet C/2013 A1 (Siding Spring), *Icarus*, *231*, 13–21, doi:10.1016/j.icarus.2013.11.028.

Morgan, D. D., O. Witasse, E. Nielsen, D. A. Gurnett, F. Duru, and D. L. Kirchner (2013), The processing of electron density profiles from the Mars Express MARSIS topside sounder, *Radio Sci.*, *48*, 197–207, doi:10.1002/rds.20023.

Pätzold, M., S. Tellmann, B. Häusler, D. Hinson, R. Schaa, and G. L. Tyler (2005), A sporadic third layer in the ionosphere of Mars, *Science*, *310*, 837–839, doi:10.1126/science.1117755.

Picardi, G., et al. (2004), Mars Express: A European mission to the Red Planet, ESA Report SP-1240, European Space Agency Publication Division, Noordwijk, Netherlands.

Restano, M., J. Plaut, B. Campbell, Y. Gim, D. Nunes, F. Bernardini, A. Egan, R. Seu, and R. Phillips (2015), Effects of the passage of Comet C/2013 A1 (Siding Spring) observed by the Shallow Radar (SHARAD) on Mars Reconnaissance Orbiter, *Geophys. Res. Lett.*, doi:10.1029/2015GL064150.

Schneider, N. M., et al. (2015), MAVEN IUVS observations of the aftermath of the comet Siding Spring meteor shower on Mars, *Geophys. Res. Lett.*, doi:10.1029/2015GL063863.

Tricarico, P., et al. (2014), Delivery of dust grains from comet C/2013 A1 (Siding Spring) to Mars, *Astrophys. J. Lett.*, *787*, L35, 5, doi:10.1088/2041-8205/787/2/L.35.

Witasse, O., J.-F. Nouvel, J.-P. Lebreton, and W. Kofman (2001), HF radio wave attenuation due to a meteoric layer in the atmosphere of Mars, *Geophys. Res. Lett.*, *28*, 3039–3042, doi:10.1029/2001GL013164.

Withers, P. (2014), Predictions of the effects of Mars's encounter with comet C/2013 A1 (Siding Spring) upon metal species in its ionosphere, *Geophys. Res. Lett.*, *41*, 6635–6643, doi:10.1002/2014GL061481.

Withers, P., M. Mendillo, D. P. Hinson, and K. Cahoy (2008), Physical characteristic and occurrence rates of meteoric plasma layers detected in the Martian ionosphere by the Mars Global Surveyor Radio Science Experiment, *J. Geophys. Res.*, *113*, A12314, doi:10.1029/2008JA013636.

Yelle, R., A. Mahieux, S. Morrison, V. Vuitton, and S. M. Hörst (2014), Perturbation of the Mars atmosphere by the near-collision with Comet C/2013 A1 (Siding Spring), *Icarus*, *237*, 202–210, doi:10.1016/j.icarus.2014.03.030.